Characterization of Polyelectrolyte Multilayers by the Streaming Potential Method

4 AUTHORS:

Zbigniew Adamczyk
Akademickie Centrum Komputerowe CYFRO…
177 PUBLICATIONS **3,696** CITATIONS

SEE PROFILE

Maria Zembala
Pedagogical University of Cracow
62 PUBLICATIONS **1,763** CITATIONS

SEE PROFILE

Piotr Warszyński
Instytut Katalizy i Fizykochemii Powierzchni i…
144 PUBLICATIONS **2,462** CITATIONS

SEE PROFILE

Barbara Jachimska
Polish Academy of Sciences
38 PUBLICATIONS **620** CITATIONS

SEE PROFILE

Characterization of Polyelectrolyte Multilayers by the Streaming Potential Method

Z. Adamczyk,* M. Zembala, P. Warszyński, and B. Jachimska

Institute of Catalysis and Surface Chemistry, Polish Academy of Science, Niezapominajek 8, 30-239 Cracow, Poland

Polyelectrolyte multilayer adsorption on mica was studied by the streaming potential method in the parallel-plate channel setup. The technique was calibrated by performing model measurements of streaming potential by using monodisperse latex particles. Two types of polyelectrolytes were used in our studies: poly(allylamine) hydrochloride (PAH), of a cationic type, and poly(sodium 4-styrenesulfonate) (PSS) of an anionic type, both having molecular weight of 70 000. The bulk characteristics of polymers were determined by measuring the specific density, diffusion coefficient for various ionic strengths, and zeta potential. These measurements as well as molecular dynamic simulations of chain shape and configurations suggested that the molecules assume an extended, wormlike shape in the bulk. Accordingly, the diffusion coefficient was interpreted in terms of a simple hydrodynamic model pertinent to flexible rods. These data allowed a proper interpretation of polyelectrolyte multilayer adsorption from NaCl solutions of various concentrations or from 10^{-3} M Tris buffer. After completing a bilayer, periodic variations in the apparent zeta potential between positive and negative values were observed for multilayers terminated by PAH and PSS, respectively. These limiting zeta potential values correlated quite well with the zeta potential of the polymers in the bulk. The stability of polyelectrolyte films against prolonged washing (reaching 26 h) also was determined using the streaming potential method. It was demonstrated that the PSS layer was considerably more resistant to washing, compared to the PAH layer. It was concluded that the experimental data were consistent with the model postulating particle-like adsorption of polyelectrolytes with little chain interpenetration. It also was concluded that due to high sensitivity, the electrokinetic method applied can be effectively used for quantitative studies of polyelectrolyte adsorption, desorption, and reconformation.

I. Introduction

Layer-by-layer deposition of anionic and cationic polyelectrolytes at solid interfaces proved to be an efficient method of preparing multilayer films of a desired composition and functionality.[1−8] The simplicity of their formation and the ability of incorporating various molecules, proteins, and colloid particles into the polymeric layer open a broad spectrum of possibilities to produce films of targeted architecture.

Numerous studies have been, therefore, performed with the aim to elucidate the basic mechanism of multilayer formation, produced usually by simply dipping the substrate into polyelectrolyte solutions of fixed ionic strength and pH value.[1−7] In contrast to the simplicity of the film preparation process, studying the film properties is a rather complicated task because of the nanometric length scale involved. As a consequence, the films have been mostly studied in the dried state by using optical methods such as ellipsometry,[6,9] X-ray reflectivity,[2,5] quartz-crystal microbalance (QCM),[4] atomic force microscopy (AFM),[4,6] scanning probe microscopy,[7] and so forth.

The in situ studies of wet films are considerably more complicated and can be performed for transparent substrates by using neutron reflectivity methods,[5] QCM,[4] total internal reflection fluorescence (TIRF),[10] tapping mode AFM,[11−13] or the scanning angle reflectometry (SAR) technique.[14]

One of the most efficient and simple techniques of measuring polyelectrolyte multilayer formation is based on electrokinetic measurements, of either electrophoretic mobility of colloid particles covered by multilayers[15,16] or streaming potential and streaming current for macrosubstrates.[9,14] As substrates in these electrokinetic studies, a fused quartz capillary[14] or a silicon wafer in the parallel-plate geometry[9] has been used. A considerable advantage of these methods is that the response of the produced multilayer to pH, ionic strength, and other parameters can easily be studied in situ.

The goal of this paper was to study by using the streaming potential technique the buildup and stability of polyelectrolyte multilayers formed on a mica surface.

---

* To whom correspondence should be addressed.

(1) Decher, G.; Honig, J. D.; Schmitt, J. *Thin Solid Films* **1992**, *831*, 210−211.

(2) Lvov, Y.; Decher, G.; Möhwald, H. *Langmuir* **1993**, *9*, 481−486.

(3) Decher, G. *Science* **1997**, *277*, 1232−1237.

(4) Lvov, Y.; Ariga, K.; Onda, M.; Ichinose, I.; Kunitake, T. *Colloids Surf., A* **1999**, *146*, 337−346.

(5) Steitz, R.; Leiner, V.; Siebrecht, R.; v. Klitzing, R. *Colloids Surf., A* **2000**, *163*, 63−70.

(6) Mendelsohn, J. D.; Barett, C. J.; Chan, V. V.; Pal, A. J.; Mayes, A. M.; Rubner, M. F. *Langmuir* **2000**, *16*, 5017−5023.

(7) Shiratori, S. S.; Rubner, M. F. *Macromolecules* **2000**, *33*, 4213−4219.

(8) Hammond, P. T. *Curr. Opin. Colloid Interface Sci.* **2000**, *4*, 430−442.

(9) Schwarz, S.; Eichorn, K.-J.; Wischerhoff, E.; Laschewsky, A. *Colloids Surf., A* **1999**, *159*, 491−501.

(10) v. Klitzing, R.; Möhwald, H. *Thin Solid Films* **1996**, *284−285,* 352−356.

(11) Rojas, O. J. In *Encyclopedia of Surface and Colloid Science*; Hubbard, A. T., Ed.; Marcel Dekker: New York, 2002; Vol. 1, pp 517−535.

(12) Schmidt, U.; Prokhorova, S.; Sheiko, S. S.; Möller, M.; Dziezok, P.; Schmidt, M. *Molecular Imaging Application Notes*; Molecular Imaging Corp.: Tempe, AZ.

(13) Percec, V.; Ahn, C.-H.; Ungar, G.; Yeardley, D. I.; Moeller, M.; Sheiko, S. S. *Nature* **1998**, *391*, 161−164.

(14) Ladam, G.; Schaad, P.; Voegel, J. C.; Schaaf, P.; Decher, G.; Cuisinier, F. *Langmuir* **2000**, *16*, 1249−1255.

(15) Donath, E.; Walther, D.; Shilov, V. N.; Knippel, E.; Budde, A.; Lowack, K.; Helm, C. A.; Möhwald, H. *Langmuir* **1997**, *13*, 5294−5305.

(16) Burke, S. E.; Barrett, C. J. *Langmuir* **2003**, *19*, 3297−3303.

II. Materials and Methods

II.A. Materials. Natural ruby mica sheets supplied by Dean Transted Ltd., U.K., were used as the substrate surfaces for polyelectrolyte deposition. Thin sheets were freshly cleaved and used in each experiment without any pretreatment.

The polyelectrolytes used were (i) the anionic poly(sodium 4-styrenesulfonate) (PSS) and (ii) the cationic poly(allylamine) hydrochloride (PAH). Both polymers had an average molecular weight of 70 000 and were purchased from Aldrich. Sodium chloride and tris(hydrooxyaminomethane) (Tris), serving in mixtures with HCl as the buffer for fixing pH, were commercial products of Sigma and Aldrich. Ultrapure water (Elix&Simplicity 185 system, Millipore SA Molsheim, France) was used for the preparation of all solutions. The Tris buffer solution of pH 7.4 was prepared by adding an appropriate amount of HCl to a Tris base solution of studied concentration.

II.B. Streaming Potential Measurements. Streaming potential was determined using a homemade apparatus described in detail previously.[17,18] The cell consisted of two polished perfluoroethylene (PTFE) blocks having two inlet and outlet compartments. Two thin substrate surfaces (mica sheets) were placed on the blocks separated by a gasket (also made of PTFE) having the thickness of 0.025 cm that served as a spacer. A parallel plate channel of the dimensions $2b \times 2c \times L = 0.025 \times 0.33 \times 3.5$ cm was then formed by clamping together the blocks with two mica sheets and the spacer, using a press under constant torque conditions. The whole setup was placed inside a grounded Faraday cage to avoid any disturbances stemming from external electric fields.

The streaming potential E_s occurring when an electrolyte solution was flowing through the cell under a regulated and constant hydrostatic pressure difference ΔP was measured using the two Ag/AgCl electrodes. These electrodes were located in two glass tubes having a direct contact with inlet and outlet compartments of the cell. A series of streaming potential measurements were done for at least five various pressures to obtain the slope of the E_s versus ΔP dependence. A Keithley 6512 electrometer having an input resistance of more than 200 TΩ was used for potential measurements. The high resistance allowed potential measurements to be carried out at practically zero current conditions. Another pair of electrodes situated outside the cell (along the flow path) was used for determination of the cell electric resistance R_c. This parameter was determined for each experiment after the streaming potential measurements. Knowing the E_s versus ΔP dependence, one can calculate the apparent zeta potential of the channel using the formula[17,18]

$$\zeta_c = \zeta_1\left[1 - \frac{16\alpha}{\pi^3} + \frac{16\alpha}{\pi^3}\frac{\zeta_2}{\zeta_1}\right] = \frac{\pi\eta}{\epsilon}\frac{E_s}{\Delta P}\frac{1}{R_c}\frac{L}{bc} = \frac{4\pi\eta}{\epsilon}\frac{E_s}{\Delta P}\lambda_{eff} \quad (1)$$

where $\alpha = 2b/2c$ is the ratio of the thickness of the channel $2b$ to its width $2c$, ζ_1 is the zeta potential of mica, and ζ_2 is the zeta potential of PTFE (side wall of the channel). The ohmic cell resistance R_c incorporating the surface conductivity effect can be expressed via the effective conductance of electrolyte in the channel λ_{eff}. This quantity was determined for each electrolyte concentration from the formula

$$\lambda_{eff} = \frac{L}{R_c \, 4bc} = \lambda_0\frac{R_{calc}}{R_{exp}}$$

where λ_0 is the bulk electrolyte specific conductivity, R_{calc} is the channel resistance expected in the case when the surface conductance is negligible, and R_{exp} represents the actual resistance of the cell. For our channel geometry $\alpha = 0.076$, the coefficient $16\alpha/\pi^3$ was equal to 0.04. This means that according to eq 1 the correction term $-(16\alpha/\pi^3)(1 - \zeta_2/\zeta_1)$ is much smaller than unity (if the mica and PTFE zeta potentials are comparable).

(17) Zembala, M.; Adamczyk, Z. *Langmuir* **2000**, *16*, 1593−1601.
(18) Zembala, M.; Adamczyk, Z.; Warszyński, P. *Colloids Surf., A* **2003**, *222*, 329−339.

The experimental procedure of determining the apparent zeta potential of polyelectrolyte-covered mica consisted of three stages:

(i) The streaming potential of bare mica was measured first by flushing the cell with pure electrolyte of fixed ionic strength and pH value.

(ii) Then, the substrate was covered in situ by a desired number of polyelectrolyte layers by filling the cell with the appropriate polymer solution (starting from PAH) of the concentration 0.5 mg/mL (500 ppm), adsorbing the polymer under no-flow conditions (30 min) and washing with pure electrolyte. The same procedure was then repeated with PSS and so forth.

(iii) Finally, without dismounting the channel, the dependence of the streaming potential on the increasing hydrostatic pressure difference ΔP was measured by flushing the cell with the pure electrolyte; knowing the slope of this dependence, the zeta potential was calculated from eq 1.

The influence of washing on the stability of multilayers for longer times, reaching 26 h, was studied in such a way that after completing a desired number of layers, the cell was flushed with the electrolyte at a constant flow rate (0.05 cm³/s) and step iii was repeated every half an hour.

II.C. Other Measurements. The zeta potential and diffusion coefficient of polyelectrolytes were determined by using a Zetasizer Nano ZS from Malvern (measurement range of 3 nm to 10 μm for zeta potential and 0.6 nm to 6 μm for particle size). The effect of bulk polyelectrolyte concentration was studied for the range of 50−2000 ppm.

The dynamic viscosity of the polyelectrolyte solutions necessary for the hydrodynamic radius calculation was measured by using a homemade capillary viscosimeter.[19]

The specific density of the polyelectrolyte crystals was determined by the density matching method. Various mixtures of 1,4-dioxane and nitrobenzene have been prepared whose density was determined by a picnometer. Then, the migration of crystals was observed under centrifugation. By repeating the procedure iteratively, the density was determined with the precision of 0.01 g/cm³.

III. Results and Discussion

III.A. Electrokinetic Characteristics of Mica. The electrokinetic characteristics of bare mica used as the substrate for polyelectrolyte adsorption have been determined according to the above-described streaming potential method. The influence of ionic strength, varied by addition of NaCl and Tris buffer, on the zeta potential of mica was evaluated. In accordance with previous measurements,[18] the effect of pH varied between 5 and 8 units was rather moderate, varying ζ_1 by a few millivolts only. In contrast, the role of ionic strength was much more significant as can be observed in Figure 1. The range of ionic strength studied was 10^{-5} to 10^{-2} M. Unfortunately, as a result of increasing electric conductivity of the electrolyte in the cell, streaming potential measurements for higher ionic strengths became less reliable. As can be seen in Figure 1, the zeta potential of mica increased monotonically with ionic strength I, assuming -85 mV for $I = 10^{-3}$ M, -67 mV for $I = 5 \times 10^{-3}$ M, and -38 mV for $I = 10^{-2}$ M. Using these data, one can estimate the effective electrokinetic charge density of the mica surface σ_0 using the Gouy−Chapman formula[20−22]

$$\sigma_0 = \left(\frac{\epsilon kT\kappa}{4\pi e}\right)\sinh\left(\frac{\zeta e}{2kT}\right) \quad (2)$$

(19) Adamczyk, Z.; Jachimska, B.; Kolasińska, M. *J. Colloid Interface Sci.*, in press.
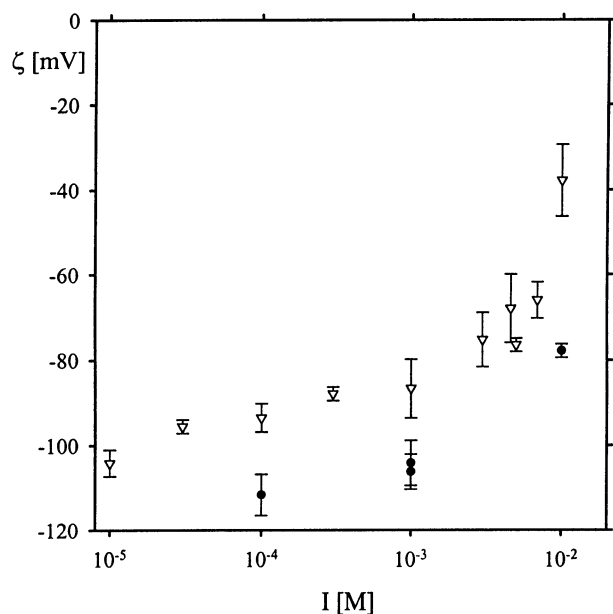(20) Gouy, G. *J. Phys.* **1910**, *9*, 457−468.
(21) Chapman, D. L. *Philos. Mag.* **1913**, *25*, 475.
(22) Adamczyk, Z.; Warszyński, P. *Adv. Colloid Interface Sci.* **1996**, *63*, 41−149.

Figure 1. Zeta potential of mica as a function of the ionic strength I regulated by NaCl ($\triangledown$) and Tris buffer pH = 7.4 ($\bullet$).

Table 1. Electrokinetic Charge of Mica

I [M]	κ^{-1} [nm]	ζ_1 [mV][a]	$\zeta_1 e/kT$	$\bar{\sigma_0}$[b]	σ_0^* [e/nm²][c]	distance between charges [nm]
10^{-3}	9.3	−85	−3.17	−4.67	−0.055	4.26
5×10^{-3}	4.2	−67	−2.7	−3.6	−0.032	5.59
10^{-2}	2.94	−38	−1.55	−1.71	−0.018	7.45

[a] ζ_1 measured by streaming potential. [b] $\bar{\sigma}_0 = \sigma_0(4\pi e/\epsilon \kappa kT)$. [c] σ_0^* = 2.1 [e/nm²] for the bare mica surface; distance between charges = 0.7 nm.

where k is the Boltzmann constant, T is the absolute temperature, e is the elementary charge, and

$$\kappa^{-1} = \left(\frac{\epsilon kT}{8\pi e^2 I}\right)^{1/2}$$

is the Debye screening length.

It was demonstrated in ref 23 by performing grand canonical ensemble simulations that despite many simplifying assumptions such as pointlike ions, lack of specific adsorption and excluded volume effects, eq 2 remains quite accurate for simple 1−1 electrolytes.

For the sake of convenience, the effective charge density on mica calculated from eq 2 for various ionic strengths is collected in Table 1 together with the average distance between charges $l_c = (e/\sigma_0)^{1/2}$.

As can be noticed, l_c increased significantly with the increase in the ionic strength from 4.26 nm for $I = 10^{-3}$ M to 7.45 nm for $I = 10^{-2}$ M. These values are much larger than the distance between charges expected for cleaved mica from crystallographic consideration,[11] equal to 0.7 nm. This means that due to accumulation of counterions at the mica surface, its natural charge is largely compensated, especially for higher ionic strength. The data shown in Table 1 suggest, therefore, that adsorption of the cationic polyelectrolyte (PAH) on mica is expected to be significantly less efficient for higher ionic strength, at least in the energetic respect.

III.B. Polyelectrolyte Characteristics in the Bulk. The specific density ρ_p of PAH and PSS in the crystalline state determined by the above-described procedure was 1.15 and 1.18 g/cm³, respectively. Thus, the molecular volume $V_1 = M/\rho_p$ Av (where M is the molecular mass of the polymer and Av is the Avogadro number) of PAH and PSS equals 101 and 98 nm³, respectively. Using these data, one can calculate the extended length of polyelectrolytes Le, a parameter of primary importance, if the effective chain cross section is estimated or known.

Previous calculations performed by Donath et al.[15] using the molecular modeling package Insight II suggested that the equivalent diameter of the PAH chain in the isotactic configuration equals 1.0 nm, which gives a cross-section area of 0.78 nm². On the other hand, in the syndiotactic configuration the effective cross-section area of the PAH chain (assumed to resemble an ellipse with the axis length equal to 0.51 and 0.87 nm) was 0.35 nm². Hence, the average value of both configurations is 0.56 nm². Analogously, the cross-section shape of the PSS chain in the more probable syndiotactic configuration was found to be 0.96 nm². Using these data, one can calculate the extended length of isolated PAH and PSS molecules as being 180 and 102 nm, respectively.

To obtain a better estimate of chain cross-section areas, we performed molecular dynamic simulations using the HYPERCHEM software package.[24] All calculations are performed using the AMBER 96[25] force field contained in the package. Partial atomic charges for polyelectrolyte ions were assigned according to the QSAR procedure[26] also contained in HYPERCHEM. The electrostatic interactions were calculated using the periodic box of dimensions $500 \times 500 \times 500$ nm and assuming the "primitive" model of electrolyte. The aqueous solvent was treated as a continuous dielectric medium with dielectric constant $\epsilon = 60$.

Snapshots of equilibrated PAH and PSS molecule configurations (fragments) in the limit of low electrolyte concentration are presented in Figure 2. As one can observe, both molecules assume a rather extended shape. This is in accordance with the Monte Carlo simulations of Stoll[27] who approximated the monomers by spheres (blobs) and used the screened Debye−Hückel electrostatic potential. Interestingly enough, the chain extension increased significantly with the molecular weight of the polymer, which was interpreted as due to increased electrostatic interaction (scaling as square of the polymerization degree).

Our simulations enabled one to calculate the effective diameter of the PAH and PSS as being 0.83 and 1.17 nm, respectively. This gives an effective chain cross-section area equal to 0.54 nm² for PAH and 1.07 nm² for PSS. As can be noticed, these values agree quite well with the calculations of Donath et al.[15] Using these cross-section areas, one can calculate the extended chain length as being 187 and 91 nm for PAH and PSS, respectively. Hence, the length-to-width ratio of the polymers λ was 225 and 78 for PAH and PSS, respectively. This axis ratio parameter is of primary importance for predicting the hydrodynamic behavior of these molecules. Another length scale of primary importance for polymer solutions is the radius of

(23) Torrie, G. M.; Valleau, J. P. *J. Chem. Phys.* **1980**, *73*, 5807−5816.

(24) *HYPERCHEM*, version 7; available from HyperCube Inc., 1115 NW 4th Street, Gainesville, FL, 32601.
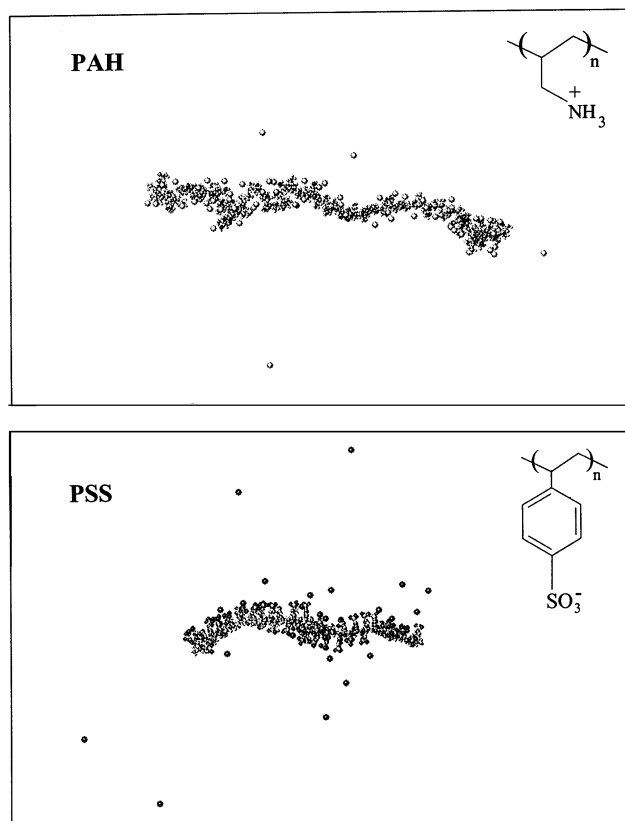(25) Cornell, W. D.; Cieplak, P.; Bayly, C. I.; Gould, I. R.; Merz, K. M., Jr.; Ferguson, D. M.; Spellmeyer, D. C.; Fox, T.; Caldwell, J. W.; Kollman, P. A. *J. Am. Chem. Soc.* **1995**, *117*, 5179−5197.
(26) Gasteiger, J.; Marsili, M. *Tetrahedron* **1980**, *36*, 3219−3228.
(27) Stoll, S. In *Colloidal Biomolecules, Biomaterials and Biomedical Applications*; Elaissari, A., Ed.; Marcel Dekker: New York, 2004; pp 211−252.

Figure 2. Snapshots of the PAH and PSS chain segments in the solution derived from numerical simulations.

Table 2. Polyelectrolyte Characteristics

property	polyelectrolyte	
	PAH	PSS
density [g/cm³]	1.15	1.18
molecular weight	70000	70000
molecular weight of monomer	93.5	206.2
number of monomers/charges	750	340
volume per molecule [nm³]	101	98.5
volume per monomer [nm³]	0.135	0.290
bare chain cross section [nm²]	0.54	1.07
extended length Le [nm]	187	91
equivalent chain diameter d_e [nm]	0.83 ± 0.07	1.17 ± 0.04
aspect ratio Le/d_e	225	78
maximum charge distance [nm]	0.87	1.20

gyration R_g of a chain that can be calculated in the limit of a rigid rod shape from the simple formula[27,28]

$$R_g = \sqrt{Le^2/12} \qquad (3)$$

Using eq 3, one obtains for R_g 54 and 26.3 nm for PAH and PSS, respectively. It also can be of interest to compare these length scales with the equivalent sphere radius

$$R_s = \sqrt[3]{3V_l/4\pi}$$

that is, the radius of the sphere having the same volume as the polymer molecule. It was found to equal 2.9 and 2.86 nm for PAH and PSS, respectively. For the sake of convenience, all the relevant parameters determined for both polymers have been collected in Tables 2 and 3.

Another important parameter characterizing polymer solution dynamics, especially the rate of deposition on

(28) Mandel, M. Some Properties of Polyelectrolyte Solutions and the Scaling Approach. In *Polyelectrolytes*; Hara, M., Ed.; Marcel Dekker: New York, 1993; pp 1–75.

Table 3. Polyelectrolyte Characteristics

property	polyelectrolyte	
	PAH	PSS
radius of gyration R_{g0} [nm]	54	26.3
radius of the equivalent sphere [nm]	2.9	2.86
diffusion coefficient[a] [cm²/s]	1.77×10^{-7}	2.07×10^{-7}
hydrodynamic radius [nm], $I = 10^{-3}$ M	13.4	11.7
diffusion coefficient[a] [cm²/s]	1.36×10^{-7}	1.80×10^{-7}
hydrodynamic radius [nm], $I = 5 \times 10^{-3}$ M	17.5	13.5
diffusion coefficient[a] [cm²/s]	1.27×10^{-7}	1.76×10^{-7}
hydrodynamic radius [nm], $I = 0.15$ M	18.7	13.8

[a] $c_p = 100$ ppm.

interfaces, is the diffusion coefficient D_p that is accessible experimentally from the dynamic light scattering measurements. However, a proper interpretation of these measurements is complicated by the fact that the D_p (evaluated from the autocorrelation function) is dependent in a strongly nonlinear manner on polymer concentration and ionic strength of the solution.[29] Because of the highly elongated shape, the pair interactions between chains become important for bulk polymer concentration above 100 ppm, especially for low ionic strength of the solution.[29] Usually, the repulsion between the chains leads to significant increase in the apparent diffusion coefficient with polymer concentration.[29,30] This effect has been confirmed experimentally in our measurements (see Table 3). We have determined for example that $D_p = 2.07 \times 10^{-7}$ cm²/s for PSS of concentration $c_p = 100$ ppm, in 10^{-3} M electrolyte solution, and 3.53×10^{-7} cm²/s for 500 ppm. It is interesting to note that with increasing electrolyte concentration the diffusion coefficient decreased systematically for both polymers. Thus, for PSS, $c_p = 100$ ppm, $D_p = 1.76 \times 10^{-7}$ cm²/s in 0.15 M electrolyte solution. It seems that these experimental data, in the dilute polymer solution limit, can well be interpreted in terms of simple hydrodynamic considerations derived for creeping flow conditions. This seems justified because flows associated with polyelectrolyte motion in solutions are characterized by very low Reynolds number $Re = LV/\nu$ (where L is the characteristic length scale of the motion, V is the characteristic velocity, and ν is the kinematic viscosity of the solution). It can be easily deduced that for the nanometer length scale involved and aqueous solution (ν of the order of 0.01 cm²/s and less) the Reynolds number remains much smaller than unity even for molecule translation velocities of the order of m/s). As a consequence of low Re number, also the relaxation time of establishing the stationary conditions of the flow distribution around a moving polyelectrolyte molecule remains exceedingly small. The relaxation time can be estimated from the simple formula

$$\tau_h = L^2/\nu \qquad (4)$$

For comparison, the mass diffusion relaxation time can be estimated from the formula

$$\tau_d = L^2/D_p \qquad (5)$$

Thus, the ratio of these two times equals D_p/ν, which is a very small quantity because, as discussed above, D_p is of the order of 10^{-7} cm²/s. In other words, because of much faster momentum diffusion in comparison with mass

(29) Koene, R. S.; Mandel, M. *Macromolecules* **1983**, *16*, 220–227.
(30) Sedlak, M.; Amis, E. J. *J. Chem. Phys.* **1992**, *96*, 826–834.

diffusion, the flow distribution is adjusting instantaneously to the polyelectrolyte molecule motion. As a consequence, its resistance coefficient could well be evaluated by using the geometrical shape of the molecule.

For bodies possessing planar symmetry, the hydrodynamic resistance matrix can be expressed in the form[31]

$$\mathbf{K_t} = \begin{vmatrix} K_{11} & & 0 \\ & K_{22} & \\ 0 & & K_{33} \end{vmatrix} \qquad (6)$$

where K_{11}, K_{22}, and K_{33} are the resistance coefficients for the motion along the corresponding axis of the Cartesian coordinate system.

The translational diffusion matrix is connected with $\mathbf{K_t}$ via the Einstein relationship

$$\mathbf{D_t} = \frac{kT}{\eta}\mathbf{K_t}^{-1} = \frac{kT}{\eta}\begin{vmatrix} 1/K_{11} & & 0 \\ & 1/K_{22} & \\ 0 & & 1/K_{33} \end{vmatrix} \qquad (7)$$

The diffusion coefficient (scalar) determined experimentally by dynamic light scattering is connected with the diagonal components of $\mathbf{D_t}$ through the relationship

$$\langle D \rangle = \frac{kT}{3\eta}\left(\frac{1}{K_{11}} + \frac{1}{K_{22}} + \frac{1}{K_{33}}\right) = \frac{kT}{6\pi\eta R_H} \qquad (8)$$

where

$$R_H = \frac{1}{2\pi\left(\dfrac{1}{K_{11}} + \dfrac{1}{K_{22}} + \dfrac{1}{K_{33}}\right)}$$

is defined as the hydrodynamic radius of the body.

The expressions for the resistance coefficients are known in an analytical form for bodies of a simple geometrical shape, for example, spheroids of arbitrary axis ratio λ, cylinders, and bent cylinders for $\lambda \gg 1$.[31] Using these expressions, one can express eq 8 explicitly as

$$\langle D \rangle = \frac{kT}{6\pi\eta}\frac{2(c_1 \ln \lambda - c_2)}{Le} = \frac{kT}{6\pi\eta R_H} \qquad (9)$$

$$R_H = \frac{Le}{2(c_1 \ln \lambda - c_2)} \qquad (10)$$

where $c_1 = 1$, $c_2 = 0$ for spheroids (in the limit of $\lambda \gg 1$); $c_1 = 1$, $c_2 = 0.11$ for cylinders (rods); $c_1 = 11/12$, $c_2 = 0.31$ for bent cylinders forming a semicircle; and $c_1 = 11/12$, $c_2 = 1.20$ for cylinders forming a circle.

R_H values calculated from eq 10 for PAH and PSS are collected in Table 4. One can notice that R_H (the resistance coefficient) for a particle having the shape of a rod is the smallest. Bending the object leads to the increase in R_H and in consequence to an increase in the hydrodynamic resistance coefficient. This allows one to interpret quantitatively the experimental data presented in Table 3, obtained for various ionic strengths of the polymer solution. In the case of low ionic strength, the polymer chain is expected to be rather extended (as the numerical simulations suggest, see Figure 2), resembling a straight rod. Indeed, the experimental R_H data for $I = 10^{-3}$ M agree almost quantitatively with the theoretical prediction for a rod. On the other hand, for increased ionic strength the

Table 4. Values of R_H [nm] Predicted from Equation 10 (100 ppm Polymer Concentration)

Shape \ Polyelectrolyte	PAH $\lambda = 225$	PSS $\lambda = 78$
Cylinder	17.6	10.7
Semicircle	20.1	12.3
Circle	24.8	16.3

Table 5. Zeta Potential ζ_p of Polymers [mV]

I [M]	polyelectrolyte PAH	polyelectrolyte PSS	I [M]	polyelectrolyte PAH	polyelectrolyte PSS
10^{-3}	75	−95	10^{-2}	50	−63
5×10^{-3}	63	−72	0.15	40	−55

polyelectrolyte molecule will be bent, and thus the experimental R_H value corresponds closely to the semicircle case. In accordance with numerical simulations, the experimental R_H value never remains smaller than the theoretical value predicted for a circle.

These observations allow one to conclude that the simple hydrodynamic model works well and can be used for prediction of polyelectrolyte chain dimensions and shapes in solutions. Hence, the extended chain length Le seems to be the most important parameter, from the hydrodynamic viewpoint, rather than the radius of gyration. This conclusion is further supported by the fact that according to generally accepted theories the radius of gyration of polyelectrolytes is expected to decrease with the increase in the ionic strength,[28] which is obviously in contradiction with observed trends.

Except for the diffusion coefficient, we have also determined the electrophoretic mobility of polyelectrolytes as a function of the ionic strength. The mobility has been converted to zeta potential by the Hückel formula. This is justified by the fact that the largest value of the $\kappa d_p/2$ parameter (characterizing the ratio of the polymer cross-section radius to the double-layer thickness) was 0.56 for PAH and 0.76 for PSS (at $I = 0.15$ M). It also is interesting to observe that for such low values of this parameter, zeta potential remains practically independent of the shape of the polyelectrolyte, either spherical or cylindrical.[32] The experimental data obtained are collected in Table 5. For $I = 10^{-3}$ M, $\zeta_p = 75$ mV for PAH and −95 mV for PSS. As can be noticed, the absolute value of the zeta potential decreased monotonically with the increase in the ionic strength attaining, for $I = 0.15$ M, 40 mV for PAH and −55 mV for PSS.

The zeta potential data are interesting because they can be used as references for the streaming potential measurements of polyelectrolyte multilayers discussed next. Moreover, they can be exploited for estimating the number of uncompensated (free) charges on the polyelectrolyte chains as a function of the ionic strength. Obviously, this charge is opposite to the mobile charge in the double layer surrounding the molecules. Because of the lack of appropriate analytical solutions for the nonlinear Poisson–Boltzmann equation in cylindrical geometry, the

(31) Happel, J.; Brenner, H. *Low Reynolds Number Hydrodynamics*; Martinus Nijhoff Publishers (Kluwer Academic): Boston, 1983; p 231.

(32) Yoon, B. J.; Kim, S. *J. Colloid Interface Sci.* **1989**, *128*, 275−288.

estimation of the mobile charge will be carried out by adopting the cylindrical capacitor model. One part of the capacitor is the polyelectrolyte chain (assumed to be a rod of the radius $d_p/2$), and the second is the double layer whose charge is assumed to be located at the distance $d_p/2 + \kappa^{-1}$. The capacity of this system is then given by the simple formula

$$C = \epsilon Le/2 \ln(1 + 2/\kappa d_p) \tag{11}$$

Knowing the capacity and zeta potential, one can calculate the number of charges per molecule from the basic relationship

$$q/e = C\zeta_p \tag{12}$$

In this way, one obtains $q/e = 115$ charges for PAH and $q/e = 82$ for PSS (at $I = 10^{-3}$ M). This is about 15% of the nominal charge for PAH and 23% for PSS (see Table 2). Similar results have been obtained for higher ionic strength as well. Analogously to the mica surface, this difference is due to compensation of the surface charge by counterions in the immobile, Stern type layer. Equation 12 gives the lowest estimate of the mobile charge as it assumes a constant capacity whereas, in reality, the capacity is increasing with increased double-layer potential (zeta potential).

Knowing the effective number of charges, one can further estimate that the average distance between the uncompensated charges equals 5.6 and 5.0 nm for PAH and PSS, respectively (for $I = 10^{-3}$ M).

III.C. Electrokinetic Characteristics of Poyelectrolyte Multilayers. Previous considerations of polyelectrolyte behavior in the bulk suggest that the molecules can be viewed as very elongated colloid particles rather than random coil (fuzzy) structures. This facilitates the analysis of possible adsorption mechanisms on the mica surface because the entropic contribution (associated with the chain conformation changes) becomes less important in comparison with the energy contribution. For polyelectrolytes, the latter is mainly governed by electrostatic chain/interface interactions with the dispersion interactions playing a less important role. Hence, a simple estimation of the energy of adsorption of polyelectrolyte molecules can be done by using the Coulomb formula

$$\phi = \frac{1}{2}\sum_{i \neq j} \sum \frac{e^2}{\epsilon d_{ij}} \tag{13}$$

where d_{ij} are the distances between the interacting (uncompensated) charges on the chain and the interface.

In practice, because of the large separation between uncompensated charges on mica and the polyelectrolyte chain, comparable with the screening length κ^{-1} (equal to 9.3 nm for $I = 10^{-3}$ M), the double sum in eq 13 can be replaced by summation among ion pairs of closest distance d_m; hence

$$\phi = \sum_{i}^{N_b} \frac{e^2}{\epsilon d_{mi}} \cong N_b \phi_0 \tag{14}$$

where $\phi_0 = e^2/\epsilon d_m$ is the energy of interaction of the ion pair forming a bond and N_b is the number of bonds. Assuming $\epsilon = 78$ and $d_m = 0.35$ nm, one obtains from eq 14 that $\phi_0 \geq 2 kT$. This value can be much larger because of the dielectric saturation effect decreasing ϵ and because of discontinuities in the water molecule distribution in the gap between ions. Thus, for PAH, assuming that the

number of bonds N_b equals half of the free charges, so $N_b = 50$, one obtains $\phi \cong -100 \, kT$ per molecule as the energy of adsorption (for $I = 10^{-3}$ M). It is expected that this value decreases for higher ionic strength due to the decrease in the number of free charges on mica.

In an analogous way, by assuming $N_b = 40$, the PAH/PSS chain electrostatic energy of interactions is expected to become larger than $-80 \, kT$.

Similar results are obtained if the interface is treated as an infinite, uniformly charged plane exhibiting the potential ζ. In this case $\phi = N_b e\zeta$ and using the data from Tables 1 and 5 one can calculate that $\phi = -180 \, kT$ for $I = 10^{-3}$ M and $\phi = -144 \, kT$ for $I = 10^{-2}$ M.

These estimates suggest unequivocally that adsorption of PAH on mica should be totally irreversible within the time scale of a typical experiment, at least for an ionic strength that is not too high. Moreover, polyelectrolyte chains will exhibit a strong tendency to adsorb side-on on a surface, minimizing the number of tails and loops. Indeed, extensive Monte Carlo simulations of Stoll[27] confirmed quantitatively this prediction. It also was predicted that the polymer coverage attained a maximum of 0.2−0.25 for ionic strength 3×10^{-2} M, and then it decreased rapidly, attaining practically zero for $I = 0.4$ M. Similarly, many experiments concentrating on measuring the adsorbed layer thickness carried out by X-ray reflectivity,[2,5] QCM, and ellipsometry[4,9] revealed that the thickness of the layer of PAH and other polyelectrolytes was of the order of the chain cross-section diameter, that is, 1−2 nm. This value increased, however, significantly when increasing the ionic strength of the electrolyte solution used for polymer deposition.

There are also a number of direct observations of the polyelectrolyte monolayers on mica, carried out by various AFM techniques, which revealed side-on adsorption of individual molecules with a small number of chain crossings (loops).[13] Interestingly enough, some of these measurements demonstrated that polyelectrolyte coverage attained a maximum of 0.2−0.25 for ionic strengths between 10^{-2} and 0.1 M.[12]

A similar value of the limiting coverage is obtained in our case by assuming a side-on adsorption of PAH on mica and neglecting, in the first approximation, the chain/chain repulsive interactions. It is postulated that one segment of the polymer, having the area $S_g = d_p d_c$ (where d_p is the polymer chain diameter and d_c is the average distance between free charges on the polymer), is blocking one charge on the mica surface. Thus, the number of adsorbed segments per unit area N_s equals the number of charges on mica, equal to $N_c = 1/d_c^2$. The polymer coverage can be then expressed by the simple formula

$$\Theta = S_g N_s = d_p/d_c \tag{15}$$

One can easily estimate that for PAH ($d_p = 0.83$ nm) $\Theta = 0.20$ for 10^{-3} M and $\Theta = 0.11$ for 10^{-2} M, which agrees well with the simulations of Stoll.[27] However, for $I < 10^{-3}$ M this limiting coverage is expected to decrease because of the chain/chain lateral interactions. On the other hand, for higher electrolyte concentrations, the dispersion interactions may increase the limiting coverage.

In view of the above considerations, one can expect that adsorption of PAH on mica is proceeding analogously to irreversible adsorption mechanisms pertinent to colloids that have been extensively studied theoretically and experimentally.[22,33−37] In particular, one can exploit the

(33) Viot, P.; Tarjus, G.; Ricci, S. M.; Talbot, J. *J. Chem. Phys.* **1992**, *97*, 5212−5218.
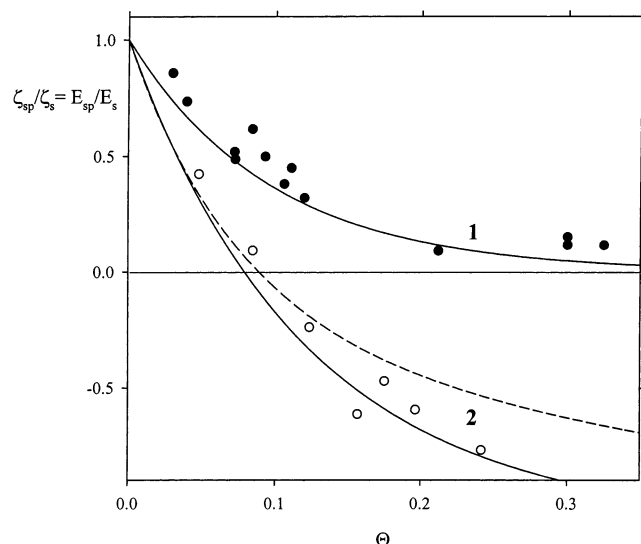
Figure 3. The dependence of the reduced zeta potential ζ_{sp}/ζ_s $= E_{sp}/E_s$ on the coverage of latex particles Θ. The points denote experimental results obtained for neutral latex particles ($\bullet$) L39, pH 7.0, and for positively charged L+57 particles ($\circ$), pH 5.8. The solid lines show the theoretical predictions derived in ref 17 for $\kappa a = 14$, and the dashed line represents the theoretical results calculated for $\kappa a = 0.2$ (pertinent to PAH adsorption).

electrokinetic data obtained for irreversible adsorption of colloid particles as reference states for interpreting the electrokinetics of polyelectrolyte deposition.

This can be done by using the calibration curves shown in Figure 3, obtained for positively charged polystyrene lattices L39 (average diameter $d = 1130$ nm) and L+57 (average diameter $d = 470$ nm) adsorbing on mica. The L39 sample was used to evaluate the effect of adsorption of neutral particles because its zeta potential can be reduced practically to zero by adjusting the pH to 7. This was revealed by electrophoretic measurements. One can observe in Figure 3 that adsorption of this neutral latex on mica resulted in reduction of the relative zeta potential ζ_{sp}/ζ_s (where ζ_{sp} is the zeta potential for particle-covered mica and ζ_s is the zeta potential for bare mica). For particle coverage $\Theta = \pi d^2 N_p/4$ (where N_p is the particle surface concentration determined by direct microscope counting[17,18]) of about 0.2, the reduced potential attained values close to zero. As a consequence, the data shown in Figure 3 can be used for calibration of other measurements when particle or polymer coverage cannot be measured directly.

The effect of decreasing ζ_{sp}/ζ_s with Θ was quantitatively interpreted in terms of a theoretical model (solid line in Figure 3) postulating a flow attenuation around particles adsorbed at the surface.[17,18] Decreased flow rate resulted in reduction of the flux (current) of ions moving out from the electric double layer near the mica surface, proportional to the factor $\mathbf{V}\rho_e$ (where $\mathbf{V}$ is the ion convection velocity and ρ_e is the local ion density in the double layer). Thus, the results shown in Figure 3 confirmed unequivocally that the electrokinetic charge at an interface can be effectively screened by purely hydrodynamic blocking of the flow by adsorbed neutral particles. In other words, a significant change in the apparent zeta potential (stream-
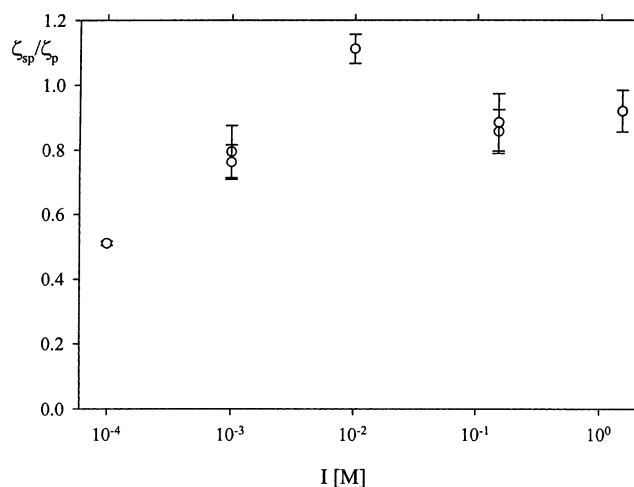
Figure 4. The dependence of the reduced zeta potential ζ_{sp}/ζ_p (where ζ_p is the bulk value of the PAH zeta potential) on the ionic strength I of the deposition bath for the first PAH layer on mica.

ing potential) of an interface can be provoked by adsorption of neutral substances.

If particles are charged oppositely to the interface, an inversion of the sign of the reduced streaming potential was observed, for coverage $\Theta < 0.1$ (see curve 2 in Figure 3). For even higher coverage, approaching 0.3, the measured value of the apparent zeta potential ζ_{sp} attained values pertinent to the particles in the bulk. This phenomenon is analogous to the overcharging effect observed often for surfactant and polymer adsorption analyzed in detail in refs 38–40.

Since this effect remains fairly independent of the thickness of the double layer κ^{-1}, the data shown in Figure 3 are of a universal character, enabling one to estimate the coverage of surfaces bearing adsorbed species of known bulk value of zeta potential, like polyelectrolytes.

These electrokinetic data obtained for PAH by the streaming potential method are shown in Figure 4. The dependence of the zeta potential of PAH-covered mica normalized to the bulk value ζ_p measured by electrophoresis is plotted as a function of the ionic strength of the solution used for polymer deposition. This parameter can be treated as the measure of the coverage degree of mica by PAH. As can be seen, this dependence exhibits a maximum in the ionic strength range 10^{-2} to 0.1 M that is in accordance with the theoretical predictions of Stoll.[27] For this ionic strength, the apparent zeta potential of the PAH layer measured by the streaming potential method attains practically its bulk value measured by microelectrophoresis. In this respect, our results deviate significantly from those obtained by Ladam et al.[14] who determined the zeta potential of a PAH-covered silica capillary to be about 3 times smaller than its bulk value. The discrepancy was probably caused by neglecting the correction to the capillary surface conductivity. Also the results obtained by Burke et al.,[16] who measured the zeta potential of PAH-covered colloid particles, deviate significantly from our results because the maximum value of the potential was only +30 mV (at pH = 7, $I = 10^{-3}$ M).

For lower ionic strength outside the above-mentioned range, the dependence of ζ_{sp}/ζ_p on the ionic strength shown

(34) Evans, J. W. *Rev. Mod. Phys.* **1993**, *65*, 1281–1329.
(35) Adamczyk, Z. *J. Colloid Interface Sci.* **2000**, *229*, 477–489.
(36) Adamczyk, Z. In *Encyclopedia of Surface and Colloid Science*; Hubbard, A., Ed.; Marcel Dekker: New York, 2001; pp 499–516.
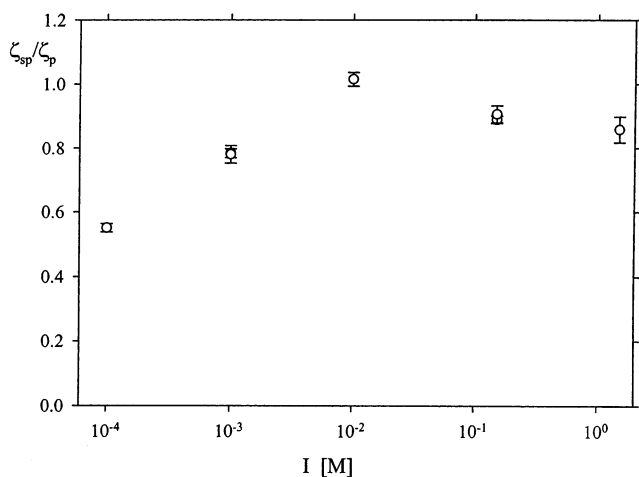(37) Adamczyk, Z. *Adv. Colloid Interface Sci.* **2003**, *100–102*, 267–347.

(38) Mateescu, E. M.; Jeppesen, C.; Pincus, P. *Europhys. Lett.* **1999**, *46*, 493–498.
(39) Nguyen, T. T.; Grosberg, A. Yu.; Shklovskii, B. I. *J. Chem. Phys.* **2000**, *113*, 1110–1125.
(40) Caruso, F.; Donath, E.; Möhwald, H. *J. Phys. Chem. B* **1998**, *102*, 2011–2016.

Figure 5. The dependence of the reduced zeta potential ζ_{sp}/ζ_p (where ζ_p is the bulk value of the PSS zeta potential) on the ionic strength I of the deposition bath for PSS on a PAH monolayer.

in Figure 4 starts to deviate significantly from unity, which indicates a decrease in the coverage of PAH in accordance with previous estimations. The results plotted in Figure 4 seem, therefore, to confirm the hypothesis of a side-on adsorption of PAH at the mica surface influenced by the ionic strength. In view of previous results for colloid particles shown in Figure 3, one also can conclude that only a part of the free charge on PAH was used to form the electrostatic bonds with the mica surface. The rest of the charge, approximately one-half, was exposed to the solution, which allowed the deposition of a consecutive layer of PSS.

The dependence of ζ_{sp}/ζ_p for the PSS layer on PAH-covered mica is shown in Figure 5. One can see that adsorption of PSS is associated with the sign inversion of the zeta potential of the bilayer. Accordingly, for an ionic strength of 10^{-2} M, ζ_{sp}/ζ_p attained maximum values close to unity, analogously to the first PAH layer. This means that the apparent zeta potential of the bilayer approached, for this ionic strength range, the zeta potential values of PSS, determined by microelectrophoresis. The appearance of the maximum in the ζ_{sp}/ζ_p versus I dependence shown in Figure 5 also suggests a side-on adsorption mechanism of the PSS molecules on the PAH layer.

From the geometrical analysis of chain sizes performed above, one can expect that on average two PSS molecules can be adsorbed at one extended PAH molecule.

The procedure of layer-by-layer deposition of PAH and PSS can be continued. Each layer deposition leads to zeta potential inversion, and these changes become quite periodic. By plotting the zeta potential of the consecutive layer against the layer number, one obtains a sawlike graph, see Figure 6, first reported by Caruso et al.[40] and Burke et al.[16] for polyelectrolyte adsorption on colloid particles. A similar graph also has been reported by Ladam et al.,[14] for PAH and PSS adsorption on fused silica. However, the amplitude of these zeta potential oscillations was 3 times smaller than that observed by us.

A possible explanation of this discrepancy is that the amplitude of the zeta potential oscillations, especially in the positive part (PAH layer formation), depends on the ionic strength of the deposition bath. For polyelectrolytes deposited from higher ionic strength ($I = 0.15$ M), the zeta potential of layers measured under an ionic strength of 10^{-3} M attained for PAH 73 mV and for PSS -88 mV, which are values almost identical to those in the bulk (see Table 5). This effect can be probably interpreted as due
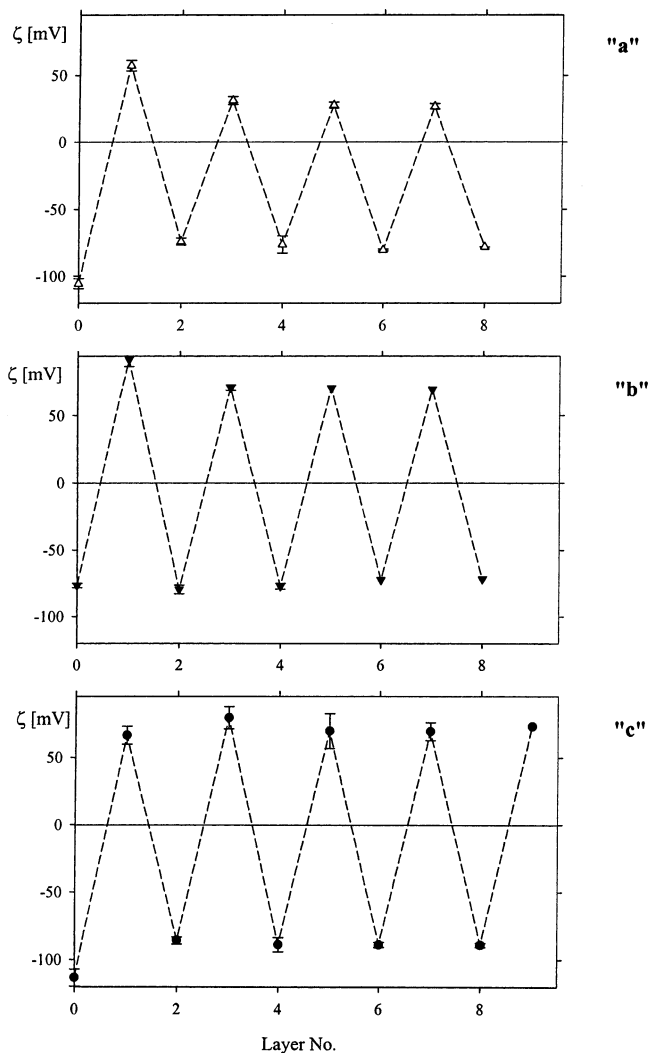

Figure 6. The dependence of the apparent zeta potential of the multilayer on the layer number, from streaming potential measurements (10^{-3} M Tris, pH = 7.4): (a) polymer deposition from a 10^{-3} M NaCl bath; (b) polymer deposition from a 5×10^{-3} M NaCl bath; (c) polymer deposition from a 0.15 M NaCl bath.

to increased density of the PAH layer on the PSS layer. The increase was caused by screening the lateral electrostatic interactions among similarly charged PAH chains. However, this can be confirmed unequivocally by precise measurements of consecutive layer thickness, which still remains a challenging task.

The results shown in Figure 6 suggest that the streaming potential method used by us enables one to characterize in situ electrokinetic properties of polyelectrolyte layers, in particular their zeta potential. Additionally, the method can be exploited for determining the stability of each monolayer against rinsing, which cannot be realized by other methods. Examples of such measurements are presented in Figures 7 and 8. The procedure of these experiments was such that upon forming the desired number of polyelectrolyte layers the channel was flushed with electrolyte (10^{-3} M Tris buffer at pH 7.4) with the wall shear rate of the flow equal to 2750 s^{-1}. At intervals of every half an hour, the streaming potential was measured for the maximum washing time reaching 26 h. As can be seen in Figure 7, the change in zeta potential of the second PSS layer was practically negligible. On the other hand, the zeta potential of the PAH-terminated layer (third) decreased significantly with time, attaining even
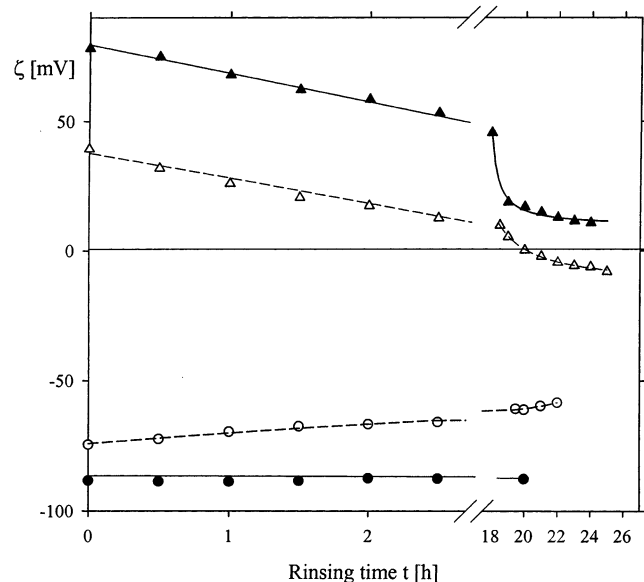
Figure 7. The dependence of the apparent zeta potential of the multilayer ζ [mV] on the rinsing time t: ($\blacktriangle$, $\triangle$) PAH and ($\bullet$, $\bigcirc$) PSS (full points and solid lines correspond to a deposition bath of ionic strength 0.15 M; empty points and dashed lines represent results obtained for a deposition bath of 10^{-3} M).
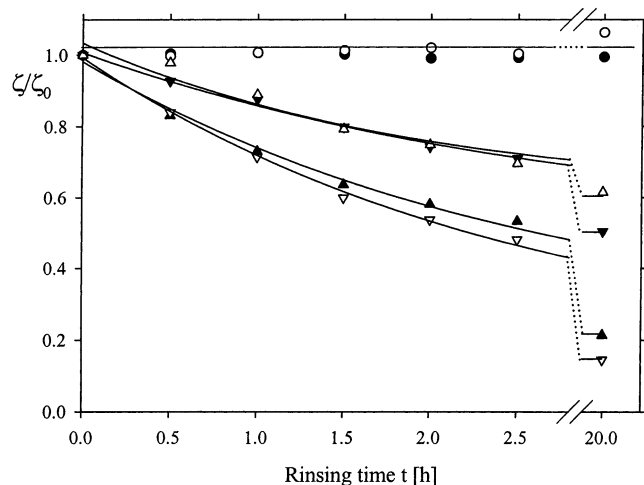
Figure 8. The dependence of the reduced zeta potential of the multilayer ζ/ζ_0 (where ζ_0 is the initial zeta potential of the layer) on the rinsing time t: ($\blacktriangle$) first PAH, ($\triangledown$) third PAH, ($\blacktriangledown$) seventh PAH, ($\triangle$) ninth PAH, ($\bullet$) second PSS, and ($\bigcirc$) fourth PSS.

negative values for prolonged washing. Moreover, in this case, the decrease in the PAH layer zeta potential was much larger when the deposition proceeded from more dilute electrolyte solutions (10^{-3} M). Also the stability of the zeta potential of a PAH layer increased with the number of deposited layers. This can be well seen in Figure 8 where the relative zeta potential ζ/ζ_0 is plotted against the rinsing time (where ζ_0 is the initial zeta potential of a layer prior to rinsing).

It is not possible, without additional measurements, to unequivocally attribute the differences in layer stability against washing shown in Figures 7 and 8 to PAH desorption processes. However, this hypothesis seems plausible because, as previously estimated, the extended length of the PAH chain (187 nm) is more than 2 times larger than for PSS (91 nm). Moreover, the flexibility of the PAH chain is much higher due to its smaller thickness and lack of a benzene ring in the chain. All this suggests that PAH adsorption on PSS may be associated with formation of a larger number of loops and tails. As a result, the adsorption energy of a significant part of the total number of adsorbed PAH molecules may be much smaller than previously estimated. This will lead to partial reversibility of PAH adsorption. An alternative explanation of the effect can be reconformation of the PAH layer.

IV. Conclusions

Measurements of diffusion coefficients of polyelectrolytes in the bulk revealed that contrary to common concepts, the hydrodynamic radius of these molecules increased with the ionic strength of the solution. These observations have been accounted for by a hydrodynamic model postulating that the extended chain length Le and the length-to-width ratio λ are the most pertinent parameters rather than the radius of gyration of the polyelectrolyte.

Estimations of the electrostatic energy of adsorption of PAH molecules on mica revealed that this process should be irreversible with chains tending to adsorb side-on at the surface. Accordingly, their deposition on surfaces is expected to proceed analogously to irreversible adsorption mechanisms pertinent to colloids. This allowed one to exploit the streaming potential data obtained for positively charged colloid lattices as reference systems for polyelectrolyte multilayer electrokinetic measurements. It was revealed that upon adsorption of the first PAH layer, the zeta potential of mica changed sign and attained a value close to the zeta potential of PAH in the bulk. This was interpreted as an indication that approximately one-half of the uncompensated charge of PAH is used to form bonds with mica. Further adsorption of consecutive PSS and PAH layers led to periodic oscillations of zeta potential.

It was also proven in the rinsing experiments that the polyelectrolyte multilayer terminated by PSS was significantly more stable than the layer terminated with PAH.

Experimental data collected in this work allow one to conclude that the streaming potential method used is a sensitive tool for characterizing in situ electrokinetic properties of polyelectrolyte layers, in particular their zeta potential. Additionally, the method can be exploited for determining the stability of each monolayer against rinsing, which cannot be realized by other methods.